

CHARACTERIZATION AND A FAST METHOD FOR SYNTHESIS OF SUB-MICRON LITHIOPHORITE

DENG-SHIU YANG AND MING-KUANG WANG*

Graduate Institute of Agricultural Chemistry, National Taiwan University, Taiwan 106

Abstract—Lithiophorite is a naturally occurring phyllosilicate which has been identified in soils and ores. Studies on a synthetic version have shed light on the conditions required for the formation of lithiophorite. In this study, we successfully prepared lithiophorite under highly alkaline conditions. In addition, we found that Li^+ , Al^{3+} and hydrothermal treatment are all necessary for the formation of lithiophorite. Lithiophorite, birnessite and Li-intercalated gibbsite were examined by infrared (IR) spectroscopy. The Mn oxide sheets of lithiophorite and birnessite were found to have quite similar structural environments. On the other hand, the $\text{LiAl}_2(\text{OH})_6$ sheets are affected more markedly by the Mn oxide sheets. After intercalation, the symmetry of the six interlayer OH groups of $\text{LiAl}_2(\text{OH})_6$ is reduced and they are divided into two groups occupying different sites, corresponding to the IR absorption bands at 3480 and 3312 cm^{-1} , respectively.

Key Words—Birnessite, Lithiophorite, Lithium-intercalated Gibbsite (LIG).

INTRODUCTION

Lithiophorite $[(\text{Al}, \text{Li})\text{MnO}_2(\text{OH})_2]$ (Post and Appleman, 1994) is a phyllosilicate which occurs naturally in soils and ores (De Villiers, 1945; Taylor *et al.*, 1964; Taylor, 1968; Larson, 1970; Ross *et al.*, 1976; Nahon *et al.*, 1984; Ostwald, 1984; Manceau *et al.*, 1990, 1992; Uzochukwu and Dixon, 1986; Golden *et al.*, 1993). It consists mainly of stacked $\text{LiAl}_2(\text{OH})_6$ sheets, instead of hydrated Na^+ cations in interlayers of birnessite, and MnO_6 octahedral sheets (Post and Veblen, 1990; Post and Appleman, 1994; Feng *et al.*, 1998, 1999).

Studies on a synthetic form provide useful information on how lithiophorite can be formed in soil or geological environments. However, reports of man-made lithiophorite are scarce. Wadsley (1950) presented the first method for preparing lithiophorite, but mentioned only that “The aluminum-lithium derivative was readily re-crystallized by heating at 433 K for three weeks in a solution containing 1% each of lithium chloride and aluminum chloride”. Giovanoli *et al.* (1973) described in greater detail their method for synthesizing lithiophorite. They mixed gibbsite, H^+ -exchanged birnessite ($\text{Mn}_2\text{O}_{13}\cdot 5\text{H}_2\text{O}$) and lithium hydroxide hydrate together and subsequently treated this admixture at 573 K for 48 h. As described by Giovanoli *et al.* (1970), a run with 20% Mn excess happened to yield almost pure lithiophorite, but it was not reproducible. Some impurities, γ - AlOOH or other unidentified compounds, were found in their products. More recently, another hydrothermal chemical process for synthesizing lithiophorite from $\text{Li}_x\text{Al}_n(\text{OH})_m^{z+}$ ion-exchanged birnessite was proposed

(Feng *et al.*, 1998, 1999). In those reports, an exchange model involving replacement of hydrated Na^+ cations by $\text{Li}_x\text{Al}_n(\text{OH})_m^{z+}$ ions in interlayers of birnessite was assumed. A 0.95/0.72 nm mixed-layered phase is thus formed. $\text{Li}_x\text{Al}_n(\text{OH})_m^{z+}$ ions are not stable under hydrothermal conditions and polymerize to form $\text{LiAl}_2(\text{OH})_6$ sheets between Mn oxide layers (Feng *et al.*, 1999).

De Jong *et al.* (1983) reported that Li^+ can promote the transition from tetrahedral $\text{Al}(\text{OH})_4^-$ to octahedral $\text{Li}_x\text{Al}_n(\text{OH})_m^{z+}$ ions. This observation was supported by our earlier study of titration of $\text{NaAl}(\text{OH})_4$ with $(\text{LiCl} + \text{HCl})$ —Li-intercalated gibbsite (LIG) can be formed even under strongly alkaline conditions (Yang, 1996). Consequently, the exchange reaction of $\text{Li}_x\text{Al}_n(\text{OH})_m^{z+}$ ions replacing hydrated Na^+ cations in interlayers of birnessite would be expected under strongly alkaline conditions.

Based on the exchange model, Feng *et al.* (1999) used birnessite, Li^+ , Al^{3+} and hydrothermal treatment at temperatures >423 K to prepare lithiophorite at a pH of ~4. Such an exchange reaction may also occur at higher pH. The objective of this study, therefore, was to prepare lithiophorite under highly alkaline conditions at 423 K. Moreover, because there is only limited information about IR characterization of lithiophorite, we also attempted to explore the structural relationships between birnessite and lithiophorite on the basis of their IR spectra.

MATERIALS AND METHODS

Chemicals

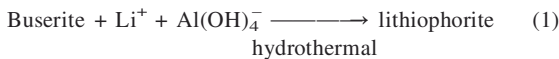
All reagent-grade chemicals were obtained commercially (Merck, Fluka or Nacalai) and used without further purification. The distilled deionized water (DDW) used in this study was obtained from a

* E-mail address of corresponding author:
mkwang@ccms.ntu.edu.tw
DOI: 10.1346/CCMN.2003.510111

Barnsted Easy Pure water purifying system and used throughout the experiment.

Syntheses

We adopted the following reaction (equation 1) to synthesize lithiophorite.



Buserite was synthesized by the method developed by Yang and Wang (2001, 2002). In the initial step, 11 g of Mn chips were dissolved with 100 mL of 6 M HClO₄. This Mn²⁺ solution was mixed with 150 mL of 19.2 M NaOH solution and a suspension of pyrochroite [Mn(OH)₂]. The volume of the pyrochroite suspension was diluted with DDW to 500 mL. Meanwhile, the concentration of NaOH was approximated to 4 M. Oxidation of the pyrochroite suspension was achieved by purging with oxygen at 273 K for 5 h. Oxygen flow rate was 2 L min⁻¹. This suspension was stirred vigorously during preparation.

Other reactants were admixed together with a buserite suspension. The admixture was made from 250 mL of birnessite suspension, 230 mL of 0.33 M NaAl(OH)₄ (4.48 g of Al reacted with water containing 20 g of NaOH, then diluted to 500 mL) and 2.5 g of LiOH·H₂O, and was heated at 425 K for 6 h. The LIG was prepared using 100 mL of 0.1 M LiOH mixed with 100 mL of 0.2 M NaAl(OH)₄ solutions (pH near 12) (Besserguenev *et al.*, 1997).

X-ray diffraction (XRD) analysis

An SRA M18XHF X-ray diffractometer operated at 50 kV and 200 mA and generating CuK α radiation was used for powder XRD analysis. Measurements were conducted in the range 5–80°2θ at a speed of 4° min⁻¹ with a step size of 0.02°2θ.

Differential thermal (DTA) and thermogravimetric (TG) analyses

A Seiko SSC 5000 thermal analyzer was used to conduct DTA and TG measurements. Samples were heated from 298 to 1273 K at a rate of 5 K min⁻¹. Meanwhile, air was purged continuously at a rate of 100 mL min⁻¹.

Scanning electron microscopy (SEM)

Scanning electron micrograph images were taken using an Hitachi S-800 Field Emission Scanning Electron Microscope equipped with Kevex Delta class 80000 EDS. The samples were coated with gold and SEM analysis conducted at an operating voltage of 20 kV.

Infrared (IR) spectrophotometric analysis

Transmission IR spectra were obtained using a Bomem model DA8.3. Middle IR spectra, from

4000 cm⁻¹ to 500 cm⁻¹, were recorded. The resolution of all spectra was 2 cm⁻¹. Sample-KBr mixtures of 200 mg (sample: KBr = 1: 400) were pressed to form a pellet of 13 mm in diameter. The IR spectra were recorded with a mercury cadmium telluride (MCT) detector. Each scan was performed 400 times. Nitrogen gas was forced into the sample chamber during scanning. For far infrared (FIR) (in the range 625–200 cm⁻¹) measurements, pellets 13 mm in diameter were prepared from 40 mg of sample-polyethylene (PE) powder mixtures (sample:PE = 1:200). The resolution was 4 cm⁻¹ and 200 scans were made. Instead of an MCT detector, a deuterated triglycine sulfate detector was employed to record the spectra. For FIR measurements, the sample chamber was evacuated.

Elemental analysis

Concentrations of Al, Li and Mn in our synthetic product were analyzed by Induced Coupled Plasma-Atomic Emission Spectrometry (ICP-AES), Jarrell-Ash, ICAP 9000.

RESULTS AND DISCUSSION

Identification of lithiophorite

Our freeze-dried synthetic product is a black powder. This powder is composed of Li, Al and Mn at an atomic ratio of 1:1.85:3.7. This differs from the ideal ratio, 1:2:3, for lithiophorite. A similar difference between polycrystalline and single-crystal lithiophorite was reported by Feng *et al.* (1999).

This synthetic lithiophorite comprises tiny platy particles, with a diameter of several hundred nanometers and a thickness of only tens of nanometers (Figure 1). The XRD patterns of the black powder and birnessite are shown in Figure 2. Compared with XRD patterns of previous reports (Feng *et al.*, 1998, 1999; Giovanoli, 1973) and JCPDS (No. 16-364), all reflections in Figure 2b can be attributed to lithiophorite [the major peaks and their indices are: 9.55: (001), 4.77: (002), 3.17: (003), 2.37: (111), 1.88: (005)]. In our work, no reflections of LiAl₂(OH)₆ClO₄·H₂O (LIG) (Besserguenev *et al.*, 1997), birnessite, or other aluminum oxyhydroxides were observed. Figure 3 shows both DTA and TG measurements. Our thermal analysis data are in good agreement with those of lithiophorite reported previously (Feng *et al.*, 1999). The DTA curve has an endothermic peak at 684 K. In addition, there was an apparent weight loss as shown in the TG curve along with the endothermic peak. The endothermic peak of 684 K and the corresponding 9.42% weight loss can be attributed to the dehydration of OH groups of LiAl₂(OH)₆ in the interlayer of lithiophorite, which accompanies a transition from lithiophorite to a Li-Al-Mn-O spinel phase (Feng *et al.*, 1999).

The IR spectrum of our synthetic Li-Al-Mn-O product is shown in Figure 4. It contains five major

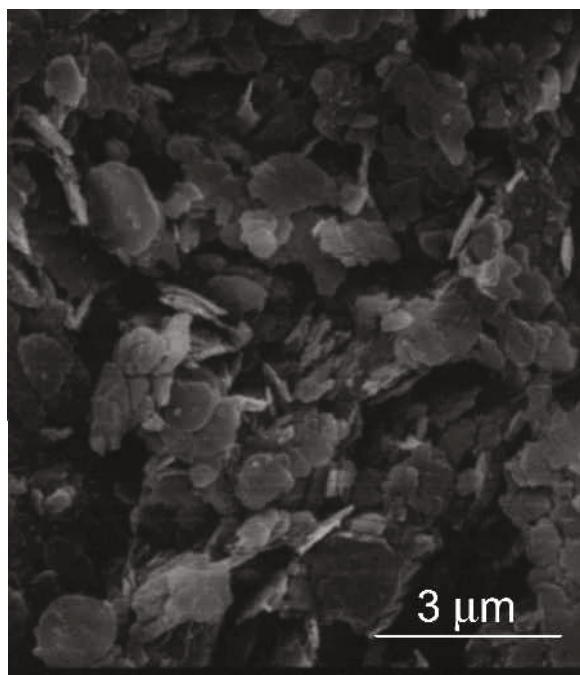


Figure 1. SEM image of lithiophorite.

absorption bands at 3480, 3312, 986, 977 and 694 cm^{-1} . The IR absorption bands at 1484 and 1438 cm^{-1} were excluded because they arose from ClO_4^- . It was previously reported that lithiophorite has four major IR bands, 3470, 3295, 985 and 703 cm^{-1} (Feng *et al.*, 1998, 1999). Our results agree very well with spectra given in

earlier reports (Feng *et al.*, 1998, 1999). Moreover, as revealed by XRD examination (Figure 1a,b), distinctions among IR spectra of LIG, lithiophorite and birnessite (Figures 4a,b,c, respectively) indicate that no impurities were found in our synthetic lithiophorite.

The results of SEM, XRD, thermal and IR analyses clearly indicate that the hydrothermal product of an admixture of birnessite, NaAl(OH)_4 and $\text{LiOH}\cdot\text{H}_2\text{O}$ is lithiophorite.

Relationships between lithiophorite, birnessite and LIG

There was no observable weight loss in lithiophorite until 684 K (Figure 3), indicating that water molecules were not present in the interlayer of lithiophorite. Evidence from the IR spectrum of lithiophorite supports this interpretation (Figure 4b). Very broad IR bands, which occur around 3600 and 1600 cm^{-1} and are assigned as water-stretching bands, were absent from the IR spectrum of lithiophorite. Previous studies regarding the assignment of gibbsite IR bands (Frost *et al.*, 1999; Wang and Johnston, 2000) offer more structural information on lithiophorite. It has recently been reported (Wang and Johnston, 2000) that the structure of gibbsite contains six unique OH groups with the hydrogen and oxygen atoms occupying C_1 sites. Owing to low site symmetry, these six OH groups had six separate IR bands at 3619, 3523, 3509, 3456, 3385 and 3361 cm^{-1} . The former three bands, 3619, 3523 and 3509 cm^{-1} , were assigned as $\nu(\text{OH})$ of intralayer OH groups. Interlayer OH groups, which form hydrogen bonds between layers, were assigned as the latter three

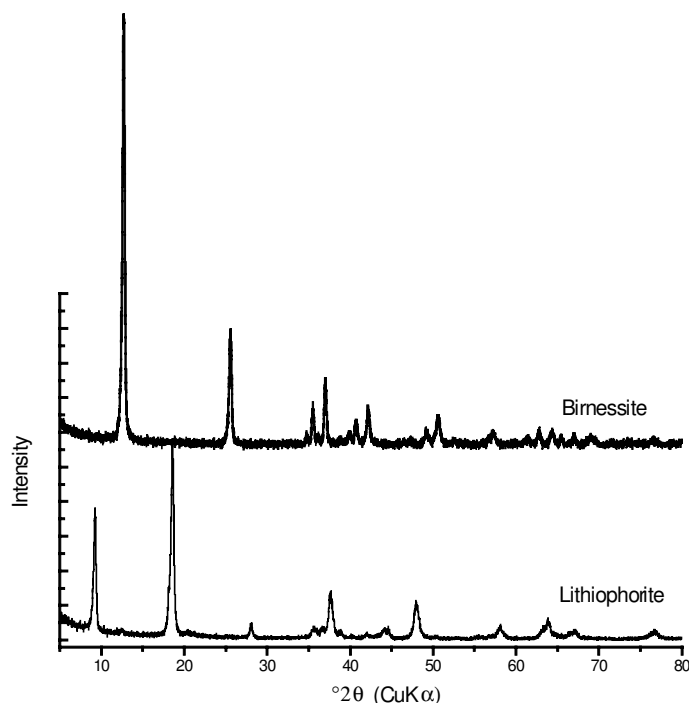


Figure 2. XRD patterns of birnessite and lithiophorite.

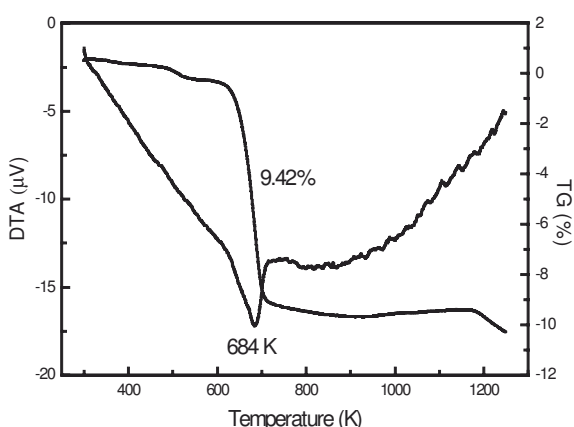
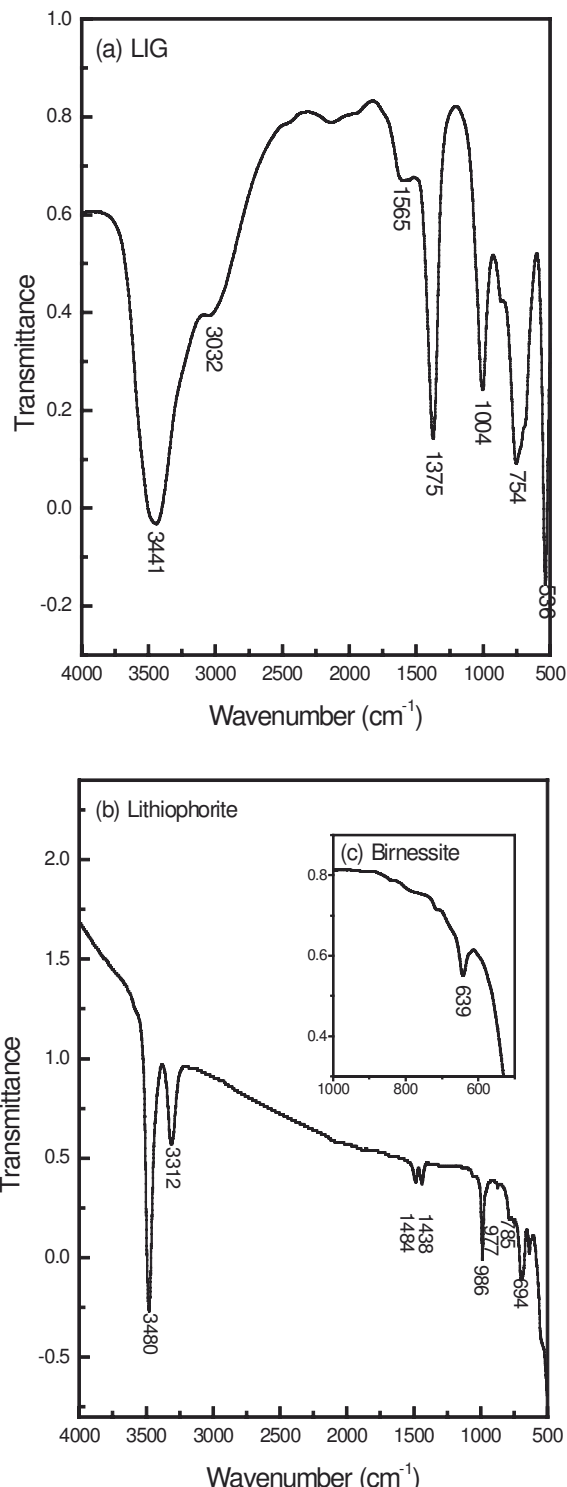


Figure 3. TG/DTA curves for lithiophorite.

$\nu(\text{OH})$ bands (Wang and Johnston, 2000). The LIG shows two broad IR bands at 3441 and 3032 cm^{-1} (Figure 4a). The ideal formula of LIG is $\text{LiAl}_2(\text{OH})_6 \cdot \text{H}_2\text{O}$ (De Jong *et al.*, 1983). In our study, X represents OH^- due to the synthesizing process we adopted. A similar IR band, at 2965 cm^{-1} , was observed in a study of $\text{LiOH} \cdot \text{H}_2\text{O}$ (Gennick and Harmon, 1975). The agreement between 3032 cm^{-1} and 2965 cm^{-1} indicates that the band at 3032 cm^{-1} can also arise from $\nu(\text{OH})$ of hydrated hydroxide anions in interlayers of our LIG. The other six OH groups on $\text{LiAl}_2(\text{OH})_6$ sheets contribute to only one IR band at 3441 cm^{-1} (Figure 4a). This suggests that the arrangement of OH groups on $\text{LiAl}_2(\text{OH})_6$ sheets of LIG is highly symmetrical and their vibration energies are degenerated. In the case of lithiophorite, two intense IR bands of 3480 and 3312 cm^{-1} are present in its spectrum (Figure 4b). The absence of OH groups with high stretching energy suggests that all OH groups in $\text{LiAl}_2(\text{OH})_6$ octahedral sheets are interlayer OH groups. They form hydrogen bonds with oxygen sites in Mn oxide sheets. Moreover, the symmetry of the six OH groups is reduced when $\text{LiAl}_2(\text{OH})_6$ sheets intercalate into the interlayer of Mn oxide sheets of birnessite. These OH groups located at two different sites are contributed by hydrogen bonds with two distinct energies. These hydrogen bonds of $\text{Mn-O} \cdots \text{H-O}$ provide most of the interlayer cohesion in lithiophorite. In particular, the intense IR band at 3312 cm^{-1} indicates that strong hydrogen bonds appear between $\text{LiAl}_2(\text{OH})_6$ sheets and Mn oxide sheets (Figure 4b). The appearance of such strong hydrogen bonds may explain why the phase transition does not occur until lithiophorite is heated above 684 K (Figure 3). In contrast, neither LIG nor birnessite has strong hydrogen bonds in their structures. Their structures are not stable when the samples are heated above 373 K (Besserguenev *et al.*, 1997).

The IR absorption bands at 1024, 969 and 914 cm^{-1} observed in gibbsite were assigned as frequencies of OH

Figure 4. IR spectra of (a) Li-intercalated gibbsite (LIG), (b) lithiophorite. In the lower spectrum, the inset demonstrates the spectrum of (c) birnessite in the range 1000–500 cm^{-1} .

deformation (Frost *et al.*, 1999). For LIG, only one OH deformation band occurs at 1004 cm^{-1} (Figure 4a). In the case of lithiophorite, its OH-deformation bands are

found at 986 and 977 cm^{-1} (Figure 4b). There is a weak shoulder IR band at 986 cm^{-1} . The trend in OH deformation among gibbsite, LIG and lithiophorite is the same as that of OH-stretching bands. The symmetry of the six OH groups of gibbsite is the lowest, whereas the OH groups of LIG are the most symmetrical. Another correlation between OH-deformation bands of LIG and lithiophorite, is that the wavenumber shifts from 1004 cm^{-1} to 986 or 977 cm^{-1} after $\text{LiAl}_2(\text{OH})_6$ sheets intercalate into Mn oxide sheets.

All IR absorption bands of lithiophorite in the range 450–800 cm^{-1} can be attributed to Mn–O vibrations. In our FIR spectra, lithiophorite resonance bands were present at 630, 538, 502, 475, 419 and 366 cm^{-1} (Figure 5a). For birnessite, IR absorption bands are present at 639, 512, 478, 417 and 360 cm^{-1} (Figure 5b). A previous study reported that the IR spectra of LiMn_2O_4 located at 619 and 513 cm^{-1} could be attributed to the asymmetric stretching modes of MnO_6 groups (Julien *et al.*, 1998). The IR bands at 630 and 502 cm^{-1} of lithiophorite and 639 and 513 cm^{-1} of birnessite are caused by the stretching modes of MnO_6 . The similarity between the IR spectra of lithiophorite and birnessite showed that the two most prominent IR bands (475 and 419 cm^{-1} in the spectrum of lithiophorite, 478 and 417 cm^{-1} in the spectrum of birnessite) are also due to the stretching modes of MnO_6 . The weak IR band at ~366 cm^{-1} (360 cm^{-1} of birnessite) can be attributed to a bending mode of Mn–O (Julien *et al.*, 1998).

In the range 800–650 cm^{-1} , no discriminative bands were identified in the middle IR spectra (Figure 4). Moreover, the FIR spectrum of lithiophorite is essentially analogous to that of birnessite except for a new IR band at 538 cm^{-1} , which is due to Al–O–Al deformations (Figure 5a) (Frost *et al.*, 1999). Therefore, the vibration mode of Mn–O of Mn oxide sheets may not be affected markedly when $\text{LiAl}_2(\text{OH})_6$ sheets intercalate into the interlayer of birnessite. Frost *et al.* (1999) attributed IR bands in the range 866–700 cm^{-1} to Al–OH–Al transitional vibrations. An IR absorption

band, at 754 cm^{-1} , present in the LIG spectrum (Figure 4a) might also be attributed to Al–OH–Al transitional vibrations. Thus, we assume that these two major IR bands, at 785 and 694 cm^{-1} , observed in the lithiophorite spectrum (Figure 4b), are due to Al–OH–Al transitional vibrations instead of Mn–O vibrations (Feng *et al.*, 1999).

CONCLUSIONS

Lithiophorite was successfully prepared under highly alkaline conditions. Together with results from a previous study (Feng *et al.*, 1999), we conclude that lithiophorite can be prepared at pH > 4. In addition, Li^+ , Al^{3+} and hydrothermal treatment (*i.e.* temperature > 423 K) are required for the formation of lithiophorite.

A comparison of IR spectra of lithiophorite, birnessite and LIG shows that Mn oxide sheets in lithiophorite and birnessite have similar structural environments. They are not affected markedly by the intercalation of $\text{LiAl}_2(\text{OH})_6$ sheets. On the other hand, the six interlayer OH groups of $\text{LiAl}_2(\text{OH})_6$ can be divided into two groups occupying different sites (*i.e.* IR absorption bands at 3480 and 3312 cm^{-1}) after they intercalate into interlayers of lithiophorite.

ACKNOWLEDGMENTS

This work was supported financially by the National Science Council, ROC, under project #NSC89-2621-B-002-006.

REFERENCES

- Besserguenev, A.V., Fogg, A.M., Francis, R.J., Price, S.J., O'Hare, D., Isupov, V.P. and Tolochko, B.P. (1997) Synthesis and structure of the gibbsite intercalation compounds $[\text{LiAl}_2(\text{OH})_6]\text{X}$ ($\text{X} = \text{Cl}, \text{Br}, \text{NO}_3$) and $[\text{LiAl}_2(\text{OH})_6]\text{Cl}_2\text{H}_2\text{O}$ using synchrotron X-ray and neutron powder diffraction. *Chemistry of Materials*, **9**, 241–247.
- De Jong, B.H.W.S., Schramm, C.M. and Farziale, V. (1983) Polymerization of silicate and aluminate tetrahedra in glasses, melts, and aqueous solutions – IV. Aluminum coordination in glasses and aqueous solutions and comments on the aluminum avoidance principle. *Geochimica et Cosmochimica Acta*, **47**, 1223–1236.
- DeVilliers, J.E. (1945) Lithiophorite from the Postmasburg manganese deposits. *American Mineralogist*, **30**, 629–634.
- Feng, Q., Honbu, C., Yanagisawa, K. and Yamasaki, N. (1998) Synthesis of lithiophorite with sandwich layered structure by hydrothermal soft chemical process. *Chemistry Letters*, 757–758.
- Feng, Q., Honbu, C., Yanagisawa, K. and Yamasaki, N. (1999) Hydrothermal soft chemical reaction for formation of sandwich-layered manganese oxide. *Chemistry of Materials*, **11**, 2444–2450.
- Frost, R.L., Kloprogge, J.T., Russell, S.C. and Szeto, J.L. (1999) Vibrational spectroscopy and dehydroxylation of aluminum (oxy)hydroxides: Gibbsite. *Applied Spectroscopy*, **53**, 423–434.
- Gennick, I. and Harmon, M. (1975) Hydrogen bonding. VI. Structural and infrared spectral analysis of lithium monohydrate and calcium and cesium and rubidium hydroxide hydrates. *Inorganic Chemistry*, **14**, 2214–2218.

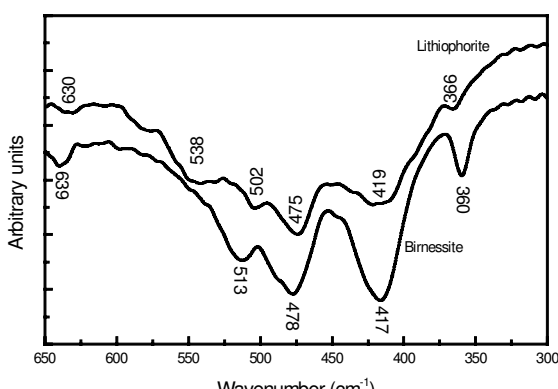


Figure 5. FIR spectra of lithiophorite and birnessite.

- Giovanoli, R., Stahli, E. and Feitknecht, W. (1970) Über oxidhydroxide des vierwertigen mangans mit schichtengitter. 1. Mitteilung: Natriummangan (II, III) manganat (IV). *Helvetica Chimica Acta*, **53**, 209–220.
- Giovanoli, R., Buhler, H. and Sokolowska, K. (1973) Synthetic lithiophorite: Electron microscopy and X-ray diffraction. *Journal de Microscopie*, **18**, 90–103.
- Golden, D.C., Dixon, J.B. and Kanehiro, Y. (1993) The manganese oxide mineral, lithiophorite, in an oxisol from Hawaii. *Australian Journal of Soil Research*, **31**, 51–66.
- Julien, C., Rougier, A., Haro-Poniatowski, E. and Nazri, G.A. (1998) Vibration spectroscopy of lithium manganese spinel oxides. *Molecular Crystals and Liquid Crystals*, **311**, 81–87.
- Larson, L.T. (1970) Cobalt- and nickel-bearing manganese oxides from the Forte Payne Formation, Tennessee. *Economic Geology*, **65**, 952–962.
- Manceau, A., Buseck, P.R., Miser, D., Rask, J. and Nahon, D. (1990) Characterization of Cu in lithiophorite from a banded Mn ore. *American Mineralogist*, **75**, 490–494.
- Manceau, A., Gorshkov, A.I. and Drits, V.A. (1992) Structural chemistry of Mn, Fe, Co, and Ni in manganese hydrous oxides: Part I. Information from XANES spectroscopy. *American Mineralogist*, **77**, 1133–1143.
- Nahon, D., Beauvais, A., Nziengui-Mapangou, P. and Ducloux, J. (1984) Chemical weathering of Mn-garnets under lateritic conditions in northwest Ivory Coast (west Africa). *Chemical Geology*, **45**, 53–71.
- Ostwald, J. (1984) Mineralogy of manganese oxides from Groote Eylandt. *Mineralium Deposita*, **48**, 383–388.
- Post, J.E. and Appleman, D.E. (1994) Crystal structure refinement of lithiophorite. *American Mineralogist*, **79**, 370–374.
- Post, J.E. and Veblen, D.R. (1990) Crystal structure determinations of synthetic sodium, magnesium, and potassium birnessite using TEM and the Rietveld method. *American Mineralogist*, **75**, 477–489.
- Ross, S.J., Jr., Franzmeier, D.P. and Roth, C.B. (1976) Mineralogy and chemistry of manganese oxides in some Indiana soils. *Soil Science Society of America Journal*, **40**, 137–143.
- Taylor, R.M. (1968) The association of manganese and cobalt in soils – further observations. *Journal of Soil Science*, **19**, 77–80.
- Taylor, R.M., McKenzie, R.M. and Norrish, K. (1964) The mineralogy and chemistry of manganese in soil Australian soils. *Australian Journal of Soil Research*, **2**, 235–248.
- Uzochukwu, G.A. and Dixon, J.B. (1986) Manganese oxide minerals in nodules of two soils of Texas and Alabama. *Soil Science Society of America Journal*, **50**, 1079–1084.
- Wadsley, A.D. (1950) Synthesis of some hydrated manganese minerals. *American Mineralogist*, **35**, 485–499.
- Wang, S.-L. and Johnston, C.T. (2000) Assignment of the structural OH stretching bands of gibbsite. *American Mineralogist*, **85**, 739–744.
- Yang, D.S. (1996) Structural properties phyllosilicates and its application to their identification in soils. Ph.D. thesis, National Taiwan University, 216 pp.
- Yang, D.S. and Wang, M.K. (2001) Syntheses and characterization of well-crystallized birnessite. *Chemistry of Materials*, **13**, 2589–2594.
- Yang, D.S. and Wang, M.K. (2002) Syntheses of birnessites by oxidizing pyrochroite with oxygen in alkaline conditions. *Clays and Clay Minerals*, **50**, 62–68.

(Received 3 January 2002; revised 6 August 2002; Ms. 617; A.E. Helge Stanjek)